Melt Polycondensation of Bisphenol A Polycarbonate by a Forced Gas Sweeping Process

Boo-Gon Woo and Kyu Yong Choi*

Department of Chemical Engineering, University of Maryland, College Park, Maryland 20742

Kwang Ho Song

Chemical Process & Catalyst Research Center, LG Chem Research Park, LG Chemical Ltd., 104-1 Moonji-dong, Yusong-gu, Taejon 305-380, Korea

Experimental and modeling studies are presented on the synthesis of bisphenol A polycarbonate at ambient pressure by a novel forced gas sweeping process. Unlike in the conventional high-vacuum melt transesterification process, the condensation byproduct (phenol) is removed from a highly viscous polymer melt in the forced gas sweeping process by forcing inert gas bubbles to flow through the polymer melt phase. As the inert gas bubbles rise in the melt phase, dissolved phenol molecules diffuse to the bubbles and are removed from the polymer melt, and the polymer molecular weight increases. To examine the feasibility of the proposed method, the effects of reaction temperature and gas flow rate on the polymer molecular weight were investigated at 260−280 °C and ambient pressure using a small semibatch laboratory reactor. It has been found that medium-range molecular weight polycarbonate can be readily prepared in a relatively short reaction time. The semibatch polymerization process is also modeled by a mass-transfer reaction model in which bubble size and bubble rising velocity are used to estimate the interfacial mass-transfer area and gas−liquid contact time. The experimental data suggest that the forced gas sweeping process can be a potential alternative to a high-vacuum melt polycondensation process for the synthesis of bisphenol A polycarbonate at ambient pressure.

Introduction

Polycarbonate (PC) is one of the most rapidly growing thermoplastic polymers, with its high heat resistance, impact resistance, optical clarity, and dimensional clarity. It is used in data storage devices, structural materials for electrical and electronic applications, automobiles, nursing bottles, and construction materials. An increasing global demand for polycarbonate (more than 10% per year) has been a driving factor for the recent increase in the global production capacity of polycarbonate, which is now more than one million tons per year.[1]

Polycarbonate has been manufactured industrially using interfacial phosgenation processes for many years. However, the high-temperature melt polymerization of bisphenol A (4,4-dihydroxydiphenyl-2,2-propane) polycarbonate (PC) is emerging as an alternative process to an interfacial phosgenation process in which the use of toxic materials might pose environmental problems. In a typical melt PC process, bisphenol A (BPA) and diphenyl carbonate (DPC) are polymerized at 260−280 °C in the presence of catalyst such as $LiOH{\cdot}H_2O$. As the polymer molecular weight increases, the melt viscosity increases rapidly, and hence, the polymerization becomes mass-transfer-controlled. Thus, high vacuum is applied to remove the phenol. The conventional melt polycarbonate process is quite similar to the melt polymerization of thermoplastic polyesters such as poly(ethylene terephthalate) (PET) in that high vacuum (1−3 mmHg or less) is applied in a multistage reaction operation to remove condensation byproducts and obtain high-molecular-weight polycarbonate. In a high-vacuum melt polycondensation process, the use of high vacuum is not economically advantageous because of high capital costs for vacuum equipment and high energy costs associated with the use of high-pressure steam for steam jets.

The melt polycondensation process is carried out in several stages under different reaction conditions to increase the polymer molecular weight. For example, monomers (BPA and DPC) are first reacted in a stirred reactor or in a series of stirred tank reactors to a low-molecular-weight prepolymer ($\bar{M}_n = 2500-5000$). Because the polycondensation reaction is reversible, phenol should be removed from the reactor to promote the forward chain-growth reaction. In a melt polycarbonate process, the polymer melt viscosity increases sharply with an increase in the polymer molecular weight, and the removal of phenol becomes difficult. Therefore, a final-stage polymerization reactor is designed to provide as large an interfacial mass-transfer area as possible to enhance the removal of phenol. For example, when a rotating-disk-type reactor is used in the finishing stage, thin polymer layers are formed at the surface of the rotating disks, and phenol is removed from the melt layers by vacuum. Thus, the interior of the reactor is designed so as to provide the shortest mass-transfer distance for phenol from the melt to the vapor phase. Because there is a limitation on polymer molecular weight that can be obtained by melt processes because of extremely high melt viscosity, solid-state polymerization might also be employed to produce high-molecular-weight injection molding grade polycarbonates.

The polymerization of bisphenol A and diphenyl carbonate is classified as a typical AABB-type conden-

* Author to whom correspondence should be addressed.

10.1021/ie000908y CCC: $20.00
Published on Web 02/14/2001

sation polymerization. In such a process, it is important during the polymerization to maintain a stoichiometric ratio of the functional end groups (A/B) to obtain a high-molecular-weight polymer. In the melt polycarbonate process carried out at 260−280 °C, diphenyl carbonate (DPC) has a moderate vapor pressure. Unless the reaction conditions and vapor-removal system are properly designed and operated, a partial loss of DPC from the reactor occurs, leading to a stoichiometric imbalance of functional end-group concentrations, which results in a low polymer molecular weight and discoloration of the final product. Thus, it is required that optimal reactor operating policies be designed and implemented.[2]

To remove volatile compounds from a polymer melt, an inert stripping gas can be introduced into a reactor at ambient pressure. The volatile compounds in the melt phase are then transferred to the gas phase and removed from the reactor. The inert gas can be introduced into the reactor without direct contact with the bulk polymer melt or it can be injected directly into the bulk polymer melt phase. The latter operation is quite similar to a polymer devolatilization process in which a stripping agent that is immiscible with the polymer is introduced into the polymeric solution. Monomers or organic solvent molecules diffuse to the surface of the gas bubbles composed mainly of the stripping agent.

Instead of using high vacuum to remove condensation byproducts, the idea of using an inert sweeping gas had been applied to polyester synthesis processes in the past. However, earlier attempts at using such methods did not lead to the development of commercial processes. In the past several years, several patents have been disclosed, notably those by Bhatia,[3−5] on the gas sweeping process for PET synthesis in which ethylene glycol is removed by an inert gas supplied to a finishing polymerization reactor. In some examples described in his patents, nitrogen gas supplied to the vapor phase of the reactor flows countercurrently to the flow of bulk polymer melt.

Although many experimental and theoretical studies have been reported on the high-vacuum melt polymerization of PET and polycarbonate,[2,7,8] very little has been reported on the mass-transfer and reaction phenomena in the gas seeping polymerization process. Woo and co-workers[6] developed a mass-transfer and reaction model to investigate the forced gas seeping process for the melt polymerization of PET. It is only recently that a patent application has been filed on the forced gas sweeping process for polycarbonate synthesis in a continuous rotating disk reactor system.[9]

In this work, we present a new experimental study on the use of inert gas in a melt polycarbonate process. Here, an inert gas such as nitrogen is supplied to a polymerization reactor and forced to flow as bubbles through a highly viscous polymer melt. The gas−liquid (melt) interfacial area provided by these bubbles offers a mass-transfer surface for the molecular transport of phenol generated by the polymerization reaction. Unlike in other similar processes (e.g., PET synthesis) reported in the patent literature where inert gas is supplied to the vapor phase (passive gas sweeping process), in the present technique, inert gas is forced to flow through a melt phase to sweep phenol more aggressively from the melt to the vapor phase (forced gas sweeping process). A dynamic mass-transfer and reaction model is also developed for an analysis of the process.

Table 1. Reaction and Jacket Temperatures at Different Gas Flow Rates

	gas flow rate (mL/s)			
	5.2	12.9	25.8	38.8
jacket temp (°C)	reactor temp (°C)			
260	258	254	247	245
280	278	276	272	269

Experimental Section

In our experimental work, the primary objective is to explore the feasibility of obtaining high-molecular-weight polycarbonate by the proposed forced gas sweeping technique. Following the polymerization procedure in ref 2, we first synthesized low-molecular-weight polycarbonate prepolymer using $LiOH \cdot H_2O$ catalyst in a stirred semibatch reactor. For the forced gas sweeping polymerization experiment, a small polymerization reactor system was designed and built. The reactor system consists of a Pyrex glass tube reactor and a glass heating jacket in which high-temperature fluid is circulated to keep the reactor temperature constant. To start a polymerization experiment, the reactor jacket temperature is raised to the desired reaction temperature. Then, a predetermined amount of polycarbonate prepolymer particles (12 g) of known molecular weight ($\bar{M}_n = 2{,}300$) is added to the glass reactor. As the reactor tube is placed in the heated glass jacket assembly, the prepolymer particles melt in about 2−3 min. Then, dehumidified and preheated nitrogen gas is supplied to the bottom of the reaction tube through a $^1/_8$-in. diameter stainless steel dip tube. Nitrogen gas injected into the reaction tube flows through the polymer melt as bubbles. The size of bubbles, the frequency of bubble formation at the tip of a dip tube, and the bubble rising velocity in the melt phase are influenced by several factors, such as the gas injection rate and melt viscosity.

For the analysis of the polymer molecular weight, a small amount of polymer sample was taken from the reactor every 30 min during the experiment. The polymer molecular weight and molecular weight distribution were measured by gel permeation chromatography (GPC) using five columns (two linear and three 500-Å columns) and a UV detector (254 nm) with tetrahydrofuran (THF) as the mobile phase.

It was observed in our experiments that the reactor temperature was slightly affected by the nitrogen gas flow rate. Table 1 shows the difference between the jacket fluid temperature and the reactor temperature. It is seen that the temperature difference tends to increase as the gas flow rate is increased. This is probably due to the loss of heat to the gas passing through the hot polymer melt. In the discussions that follow, we will use the jacket temperature to represent the reaction temperature.

Experimental Observations

Before we present the experimental results of polymerization, we will present some interesting observations made during the reaction experiments.

As the reactor temperature is raised to above the polymer melting point, polymerization begins even before the injection of nitrogen gas, as indicated by the formation of small phenol bubbles. This occurs because the concentration of reactive end groups in the low-molecular-weight prepolymer is quite high. Nucleated

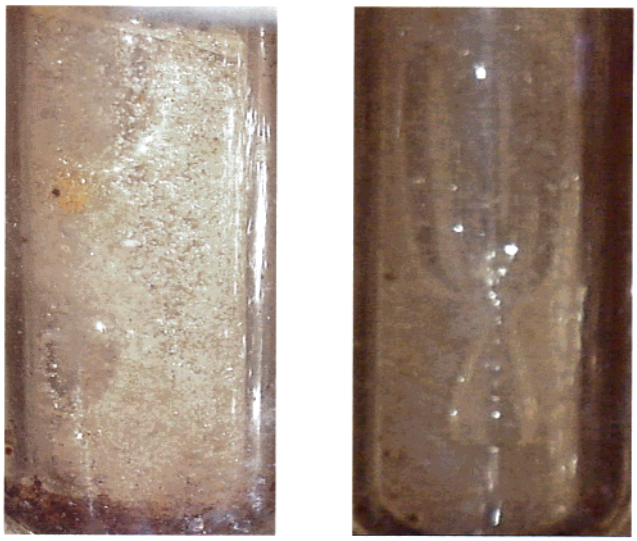

(a) (b)

Figure 1. (a) Nitrogen gas bubbles (large bubbles) and nucleated phenol bubbles (small bubbles) at low conversion; (b) gas bubbles at high conversion.

phenol bubbles of about 1-mm diameter quickly saturate the reactor, and the polymer melt looks like a boiling liquid. At ambient pressure, most of these phenol bubbles stay in the reactor. In our separate experiment without the use of either vacuum or nitrogen gas, it was found that the reaction reached an equilibrium, and the increase in polymer molecular weight was almost negligible, indicating that high-molecular-weight polymer can not be obtained unless phenol is removed from the reactor.

Heated nitrogen gas is supplied to the reactor after the prepolymer particles melt completely. At the beginning of a polymerization experiment, the melt viscosity is relatively low, and a swarm of small nitrogen bubbles rises rapidly in the melt phase. These nitrogen gas bubbles cause intense mixing of the melt in the reactor and promote the upward movement of phenol bubbles, which then burst at the surface of the melt. At the same time, dissolved phenol diffuses into the gas bubbles. Figure 1a shows a snapshot of the reactor at low conversion. Notice that nearly spherical nitrogen gas bubbles (large bubbles) rise in the sea of small nucleated phenol bubbles. Also notice in Figure 1a that the nitrogen gas bubbles are far larger than the gas injection tube diameter. With an increase in conversion, the amount of nucleated phenol bubbles decreases significantly.

As conversion increases, the melt viscosity increases rapidly, the bubbles become larger (Figure 1b), and the bubbles detach from the gas injection nozzle much less frequently. Thus, the number of nitrogen gas bubbles in the polymer melt decreases. Figure 2 shows the frequency of bubble detachment from the injection nozzle. The symbols and the line are the experimental data and model calculations, respectively. The entire experiment was videotaped, and the bubble detachment frequency was measured by visual observation. Notice that the bubble detachment frequency decreases significantly because the bubbles inflate as the polymer molecular weight increases.

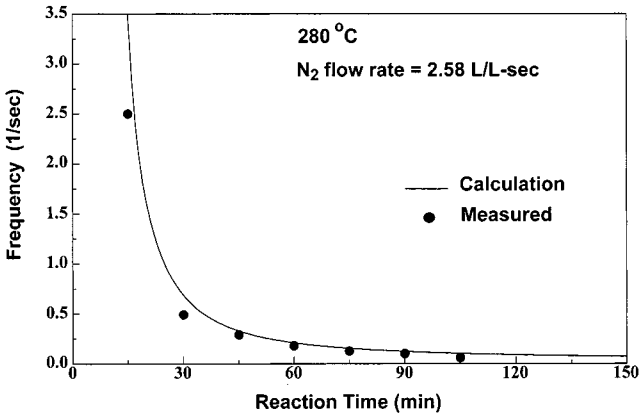

Figure 2. Frequency of bubble detachment: symbols, measurements; lines, calculations.

When a large bubble rose and burst at the top of the reactor, a loud popping sound was heard. It was observed at very high melt viscosity that a bubble formed at the tip of the tube inflated to almost the size of the reaction tube diameter. The bubble detached from the tube tip and rose as a cylindrical slug in the melt phase, pushing the polymer melt around the bubble toward the reactor tube walls. As these large bubbles burst at the top of the reactor and the polymer melt flowed downward along the reactor walls, injected nitrogen gas passed through the reaction tube without forming bubbles until the melt volume was recovered. In Figure 1b, we can see a smaller bubble still attached to the injection nozzle. It inflates to the size of an already-detached bubble immediately above it before being detached from the nozzle.

Polymerization Process Model

For the analysis of mass-transfer and reaction phenomena, we develop a mathematical reaction model. Although some side reactions might occur, we consider only the main polycondensation reaction between hydroxyl and phenyl carbonate groups as follows

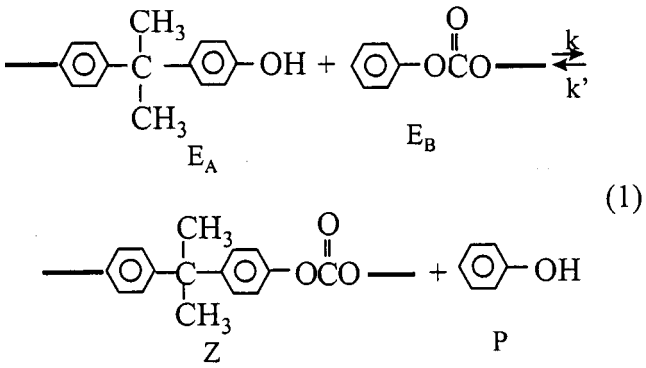

(1)

where E_A and E_B denote hydroxyl and phenyl carbonate groups, respectively. Z is the polymer repeat unit, and P is phenol. The reaction rate is expressed as

$$r_p = k[E_A][E_B] - k'[Z][P] \qquad (2)$$

The above reaction occurs even in the absence of added catalyst.[7,8] The effective forward reaction rate constant in the presence of catalyst (e.g., $LiOH \cdot H_2O$) is expressed as[8]

$$k = k_u + k_c[C^*] \tag{3}$$

where $[C^*]$ is the catalyst concentration, k_u is the rate constant for the uncatalyzed polycondensation reaction, and k_c is the rate constant for the catalyzed reaction. The reverse reaction rate constant is expressed in a similar form. The forward and reverse reaction rate constants for the uncatalyzed polycondensation are[8]

$$k_u = (5.180 \pm 0.170) \times 10^8 \exp[(-25\,290 \pm 1010)/RT]\ (\mathrm{cm^3\ mol^{-1}\ s^{-1}}) \tag{4}$$

$$k'_u = (3.380 \pm 0.377) \times 10^{16} \exp[(-45\,030 \pm 2430)/RT]\ (\mathrm{cm^3\ mol^{-1}\ s^{-1}}) \tag{5}$$

The catalyzed reaction rate constants are

$$k_c = 1.603 \times 10^{13} \exp[-13900/RT]\ (\mathrm{cm^6\ mol^{-2}\ s^{-1}}) \tag{6}$$

$$k'_c = 1.340 \times 10^{12} \exp[-12090/RT]\ (\mathrm{cm^6\ mol^{-2}\ s^{-1}}) \tag{7}$$

In the above expressions, the activation energies are in calories per mole, and the gas constant $R = 1.987$ cal $\mathrm{mol^{-1}\ K^{-1}}$.

When an inert gas is injected into a polymer melt through a nozzle, bubbles are formed and rise in the melt phase. Then, phenol formed by the polymerization reaction diffuses from the polymer melt into the gas bubbles. The size of the bubbles and the number of bubbles depend mostly upon the gas flow rate and melt viscosity. The molar transfer rate of phenol from the polymer melt phase to the nitrogen gas bubbles can be represented by

$$N_p = (k_L a)_L([P]_L - [P]^*_L) = (k_L a)_G([P]^*_G - [P]_G) \tag{8}$$

where $(k_L a)_L$ and $(k_L a)_G$ are the mass-transfer coefficients of phenol in the polymer melt phase and the nitrogen gas phase, respectively (a = specific interfacial surface area per liquid volume). $[P]_L$ ($[P]_G$) is the concentration of phenol in the liquid phase (gas bubble phase), and $[P]^*$ is the corresponding equilibrium concentration at the gas−liquid interface. The concentrations of phenol at the gas−liquid interface are related by the equation

$$[P]^*_G = K[P]^*_L \tag{9}$$

Then, from eqs 8 and 9, we obtain

$$[P]^*_L = \frac{(k_L a)[P]_L + (k_L a)_G[P]_G}{(k_L a)_L + K(k_L a)_G} \tag{10}$$

The molar mass-transfer rate of phenol per unit interfacial surface area is expressed as

$$N_p = \frac{K[P]_L - [P]_G}{\dfrac{1}{(k_L a)_G} + K\dfrac{1}{(k_L a)_L}} \tag{11}$$

If the mass-transfer resistance in the nitrogen gas phase is much smaller than the mass-transfer resistance in the polymer melt phase, the above equation is reduced to

$$N_p = (k_L a)_L\left([P]_L - \frac{1}{K}[P]_G\right) \tag{12}$$

For a semibatch melt polycondensation reactor in which nitrogen gas is continuously injected into a prepolymer melt, the mass balance equation for phenol is

$$\frac{d[P]_L}{dt} = r_p - (k_L a)_L\left([P]_L - \frac{1}{K}[P]_G\right) \tag{13}$$

where r_p is the rate of phenol formation. If the volume of nitrogen gas bubbles (i.e., gas holdup) in the melt is assumed to be constant, the mass balance equation for phenol in the gas phase is given by

$$V_G \frac{d[P]_G}{dt} = V_L(k_L a)\left([P]_L - \frac{1}{K}[P]_G\right) - Q_G[P]_G \tag{14}$$

where Q_G is the nitrogen gas flow rate, V_L is the melt phase volume, and V_G is the gas (bubble phase) volume. In deriving eqs 13 and 14, it was assumed that both the melt phase and the bubble phase are well mixed and that the gas composition in each bubble is same.

If the bubbles are spherical and of uniform size, the total specific interfacial surface area is $N_b S^*_G/V_L$, where N_b is the total number of gas bubbles in the reactor and S^*_G is the surface area of a gas bubble. The mass-transfer coefficient is estimated using penetration theory as $k_L = 2\sqrt{D_p/\pi\theta}$, where D_p is the diffusivity of phenol in the polymer melt and θ is the time that a fluid element in the melt phase is in contact with a gas phase at the gas−liquid interface.

The formation of gas bubbles and their behavior in viscous liquids have been the subject of studies by many researchers in many different technical fields (e.g., fermentation, drying of liquid foodstuffs, wastewater treatment, polymer devolatilization, etc.). Predictions of bubble size, bubble growth, and bubble rising velocity in a highly viscous or viscoelastic fluid are important for process design. However, such phenomena are quite complex, and not much has been reported on the formation and movement of bubbles in high-viscosity polymer melts. In addition, no report is available on bubble formation and growth in a reactive polymer melt where the melt viscosity increases with conversion or time.

To model the gas sweeping process that we consider in this work, it is necessary to estimate the effective interfacial mass-transfer area provided by the gas bubbles. As the gas flow rate is increased to a certain point, bubble formation is hindered by the presence of preceding bubbles, and bubble size increases as a function of gas flow rate rather than orifice size. Bubble size is also strongly dependent on the fluid viscosity. In our experiments, the gas flow rates employed are such that bubbles are far larger than the diameter of the gas injection nozzle (see Figure 1). Using the equation developed by Davidson and Schüler[10] for very low Reynolds number fluids (Re < 0.002), we can estimate the bubble diameter (d_b) as

$$d_b = 2.313\left(\frac{\mu Q_G}{\rho g}\right)^{1/4} \tag{15}$$

where Q_G is the volumetric gas flow rate ($\mathrm{cm^3/s}$), μ is the melt viscosity (g $\mathrm{cm^{-1}\ s^{-1}}$), ρ is the melt density (g/

cm^3), and g is the gravitational acceleration constant (980 cm/s^2). In deriving the above equation, Davidson and Schüler[10] assumed that (i) the bubble is spherical throughout formation, (ii) the liquid surrounding the orifice is at rest when the bubble starts to form, (iii) the motion of the gas bubble is not affected by the presence of another bubble immediately above it, (iv) the momentum of the gas is negligible, and (v) the bubble is at all instants moving at Stokes velocity appropriate to its size. In our polymerization system, some of these assumptions might not be exactly applicable. For example, Davidson and Schüler[10] tested the validity of the above equation for fluids with viscosities up to 1040 cp, which is far smaller than the viscosity of the polycarbonate melt in our polymerization system. Also, according to our experimental observations, bubbles detached from the tip of a gas injection tube are nearly spherical at low melt viscosities (i.e., during initial reaction period), but as the melt viscosity increases because of polymerization, the bubbles are inflated and become elongated in the vertical direction (flow direction) (Figure 1b). As such large bubbles rise and burst, the polymer melt flows downward by gravity along the reactor walls. Until a pool of polymer melt is formed again at the bottom of the reaction tube, the injected gas passes through the reactor without forming bubbles. In our model simulations, however, bubbles are approximated as spheres during their formation, growth (at the nozzle tip), and rise in the polymer melt. If the calculated bubble diameter exceeds the reaction tube diameter, the equivalent cylindrical bubble slug is assumed to estimate the effective interfacial mass-transfer area.

Equation 15 also indicates that the bubble size increases with an increase in melt viscosity. For example, according to eq 15, a 10-fold increase in melt viscosity or gas flow rate results in about a 78% increase in bubble diameter. At a fixed gas flow rate, the gas bubble size increases as the polymer melt viscosity increases with reaction. Polycarbonate melt viscosity data are scarce. Schnell[11] reported polycarbonate melt viscosity versus molecular weight data at 280 and 302 °C. These data were fitted by the equation

$$\ln \mu = \left(393.15 - \frac{2.43 \times 10^5}{T}\right) + \left(\frac{2.49 \times 10^4}{T} - 39.8\right) \ln \bar{M}_w \quad (16)$$

where T is the melt temperature in Kelvin and $\bar{M}_w$ is the weight-average molecular weight of the polycarbonate. Figure 3 shows the data and the predictions of eq 16.

We further assume that the increase in the bubble size due to the diffusion of phenol from the melt phase to the nitrogen bubbles is negligible because the bubble−melt contact time is quite small and the amount of phenol in the fast-rising bubbles is also quite small. We also ignore the change in bubble size due to bubble breakup or coalescence. In the experimental reactor that we used, no bubble breakup or coalescence was observed.

Another important variable for the estimation of the bubble surface area and contact time is the bubble rising velocity. For a power-law fluid, Chhabra[12] reports that, depending upon the values of power-law flow index (n) and the gas volume fraction, the rise velocity of a bubble swarm might be greater or smaller than the velocity of a single bubble. At high reaction temperatures (e.g., 280 °C), molten polycarbonate is essentially a Newtonian liquid with negligible viscoelastic effects.[11] To calculate the bubble rising velocity, we use the equation proposed for a viscous liquid by Snabre and Magnifotcham[13]

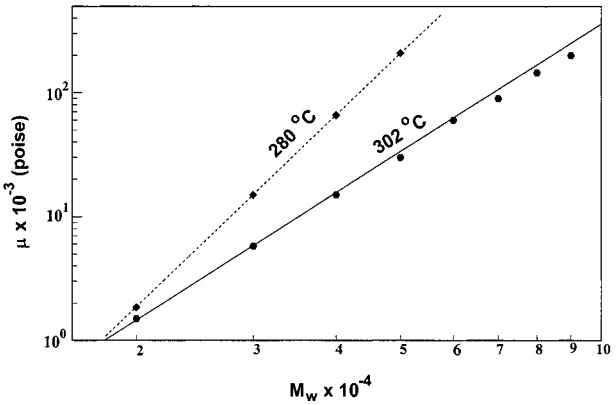

Figure 3. Melt viscosity of polycarbonate vs molecular weight.

$$u_b = \left[\frac{2 d_b g}{C_d}\left(1 + \frac{Q_G d_b}{u_b V_G^*}\right)\right]^{1/2} \quad (17)$$

where d_b is the bubble diameter (cm), V_G^* is the volume of a bubble (cm^3), and C_d is the drag coefficient ($C_d = 16/Re + 1$).

The average bubble residence time or contact time (θ) and the number of bubbles (N_b) with an average residence time of θ are estimated using the equations

$$\theta = \frac{V_L(1 + \epsilon_G)}{u_b S_R} \quad (18)$$

$$N_b = \frac{Q_G \theta}{V_G^*} \quad (19)$$

where V_L and S_R represent the polymer melt volume and the cross-sectional area of the tube reactor, respectively. The frequency of bubble detachment is given by N_b/θ. The fractional gas holdup ($\epsilon_G = V_G/V_L$) in the polymer melt is estimated by the correlation developed for a bubble column by Godbole et al.[14] for a highly viscous fluid

$$\epsilon_G = 0.239(u_b \times 10^{-2})^{0.634} D_R^{-0.5} \quad (u_b \text{ in meters per second and } D_R \text{ in meters}) \quad (20)$$

where D_R is the reactor diameter. In our model, we assume that the contact time is approximately equal to the average residence time of a bubble rising in the melt phase. The total mass-transfer area can be calculated by multiplying the number of bubbles by the specific surface area of a bubble.

Assuming that the polymer chain length does not affect the reactivity of the functional groups, we can derive the reactor model equations as follows:

$$\frac{d[E_A]}{dt} = \frac{d[E_B]}{dt} = -r_p \quad (21)$$

$$\frac{d[Z]}{dt} = r_p \quad (22)$$

$$\frac{d[P]_L}{dt} = r_p - (k_L a)\left([P]_L - \frac{1}{K}[P]_G\right) \quad (23)$$

$$V_G\frac{d[P]_G}{dt} = V_L(k_L a)\left([P]_L - \frac{1}{K}[P]_G\right) - Q_G[P]_G \quad (24)$$

In deriving the above model equations, we assume that the melt phase volume remains constant during the polymerization process, even with the loss of the reaction byproduct, phenol. (In our experiments, the amount of phenol removed from the tube reactor after the degree of polymerization is increased from 9 to 50 is about 0.5 mL from the initial 12 g of prepolymer.) The degree of polymerization is given by

$$\bar{X}_n = 1 + \frac{2[Z]}{[E_A] + [E_B]} \quad (25)$$

The rate constant in the above model is the effective rate constant in which the catalyst concentration effect is incorporated.

The degree of polymerization ($\bar{X}_n$) of the prepolymer used in our experiments is 9 ($M_n = 2300$), and the initial end-group concentrations in the prepolymer are $[E_A] = 0.442 \times 10^{-3}$ mol/cm^3, $[E_B] = 0.570 \times 10^{-3}$ mol/cm^3, $[Z] = 3.663 \times 10^{-3}$ mol/cm^3, and $[P] = 0.013 \times 10^{-3}$ mol/cm^3. The interfacial phase equilibrium parameter, $K = 5.0 \times 10^{-3}$, was used in the model simulations.

Results and Discussions

Two experimental runs were first done to investigate the feasibility of obtaining relatively high-molecular-weight polycarbonate by the forced gas sweeping process. Figure 4a shows the degree of polymerization ($\bar{X}_n$; molecular weight of a repeat unit = 254) profiles with reaction time at 260 and 280 °C (jacket temperatures) and at a nitrogen gas flow rate of 25.8 mL/s [specific gas flow rate = 2.58 L (L of melt)$^{-1}$ s^{-1}]. The symbols are experimental data, and the lines are the model simulation results. First, it is clearly seen that the polymer molecular weight increases surprisingly rapidly from 2300 ($\bar{X}_n = 9$) to 8000 ($\bar{X}_n = 32$) at 260 °C and 14000 ($\bar{X}_n = 55$) at 280 °C in 150 min. For comparison, the results of high-vacuum semibatch polymerization experiments are shown in Figure 5.[2] Here, the reaction temperature and pressure were changed in five different stages. Figure 5 shows that the polymer molecular weight reaches from ~2000 to 5000 (M_n) in 1 h at 280 °C and 10 mmHg (stage 5). The same concentration of catalyst was used in both experiments. The results shown in Figure 4 clearly suggest that the proposed forced gas sweeping process is quite effective in obtaining medium-range molecular weight polycarbonate in a relatively short reaction time.

In our model simulations, we observed that the model prediction results were quite sensitive to the diffusivity of phenol in the melt phase. In molten polyethylene-(terephthalate), which is similar to molten polycarbonate, the reported value of the diffusivity of ethylene glycol is 1.66×10^{-4} cm^2/s.[15] The diffusivity of phenol in a polycarbonate melt has not been reported in the literature. When a constant diffusivity was used, poor agreement was observed between experimental data and model prediction results. For example, Figure 4b shows that, when the diffusivity used for the simulations at 280 °C is used for the simulation at 260 °C, a poor fit of the data is obtained. Thus, at each temperature, the diffusivity value was adjusted to match the

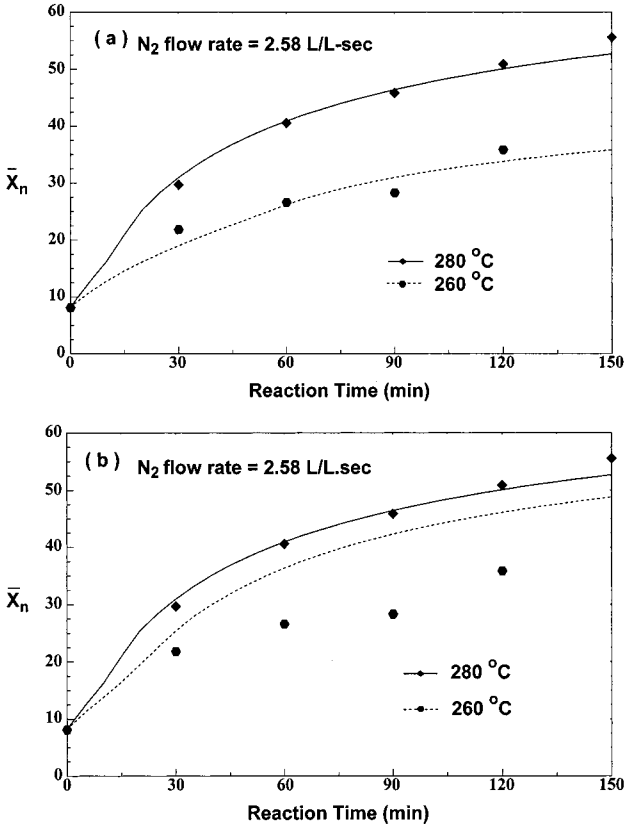

Figure 4. Effect of reactor temperature on the degree of polymerization: (a) simulations with temperature-dependent diffusivity of phenol; (b) simulations with constant diffusivity of phenol.

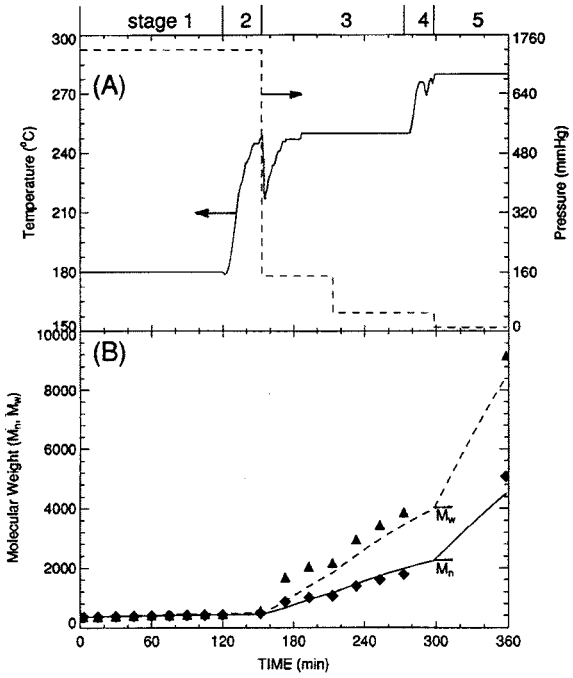

Figure 5. Polycarbonate molecular weight in a multistage melt polymerization.[2]

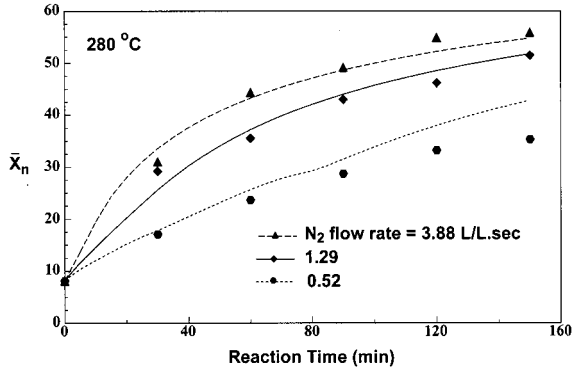

Figure 6. Effect of nitrogen gas flow rate on the degree of polymerization.

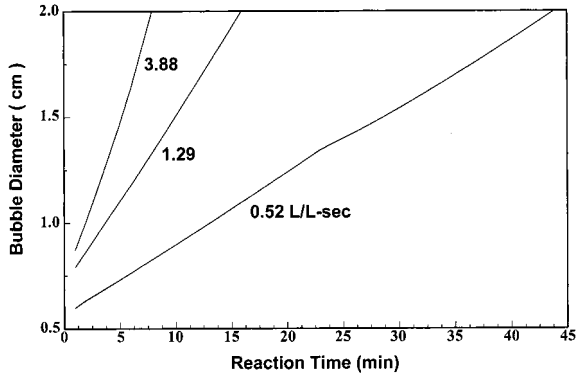

Figure 7. Calculated bubble diameter profiles at different gas flow rates.

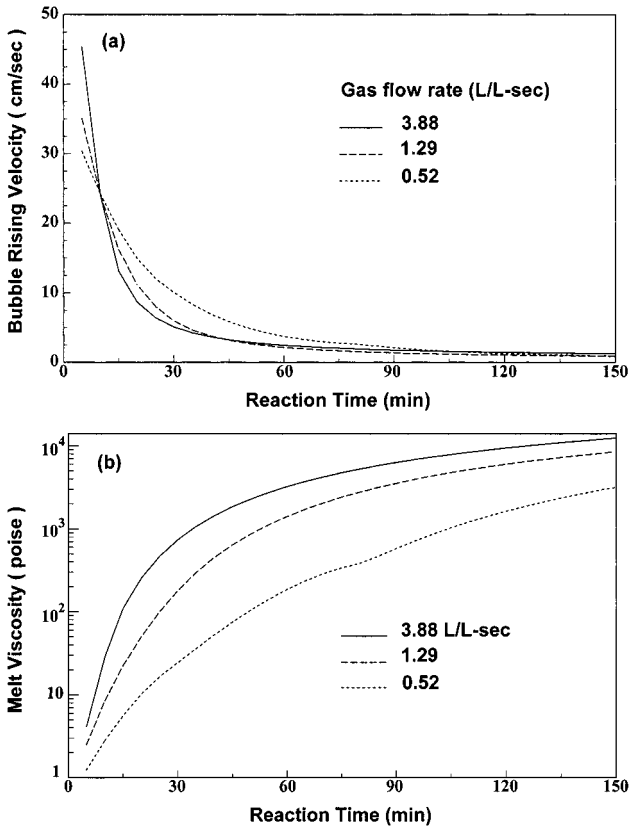

Figure 8. (a) Bubble rising velocity; (b) melt viscosity at different nitrogen flow rates (calculation).

simulation results to the corresponding experimental data [D_p(280 °C) = 7.9 × 10^{-5} cm^2/s, D_p(260 °C) = 9.5 × 10^{-7} cm^2/s].

The effect of the nitrogen gas flow rate on the polymer molecular weight is illustrated in Figure 6. Here, the symbols are experimental data, and the lines are model simulation results. It is seen that higher gas flow rates give rise to higher polymer molecular weights. However, the effect of increasing the gas flow rate on the polymer molecular weight diminishes as the gas flow rate is increased further.

Figure 7 shows the calculated bubble diameter during polymerization. It is seen that the gas bubble diameter reaches its maximum (of 2 cm, which is approximately equal to the reactor tube diameter) in about 45 min at a low gas flow rate (0.52 L L^{-1} s^{-1}), but it takes much less time at a higher gas flow rate (3.88 L L^{-1} s^{-1}). Figure 8a shows the computed bubble rising velocity, and Figure 8b shows the melt viscosity values during the polymerization at different nitrogen gas flow rates. It is seen that the gas bubble rising velocity at high gas flow rates deceases very rapidly as the conversion and melt viscosity increase. At high gas flow rates (e.g., 3.88 L L^{-1} s^{-1}), the melt viscosity increases by nearly 3 orders of magnitude in about 30 min of reaction time.

The variations in the specific mass-transfer area (calculated) with degree of polymerization during the polymerization are shown in Figure 9 for three different gas flow rates. Also shown are the sketches of the bubbles/slugs observed experimentally at different reaction stages. When the conversion is low, the specific surface area is large because the number of bubbles is large and the bubbles are small. As the conversion or molecular weight increases, the number of bubbles decreases significantly, and the bubbles become larger,

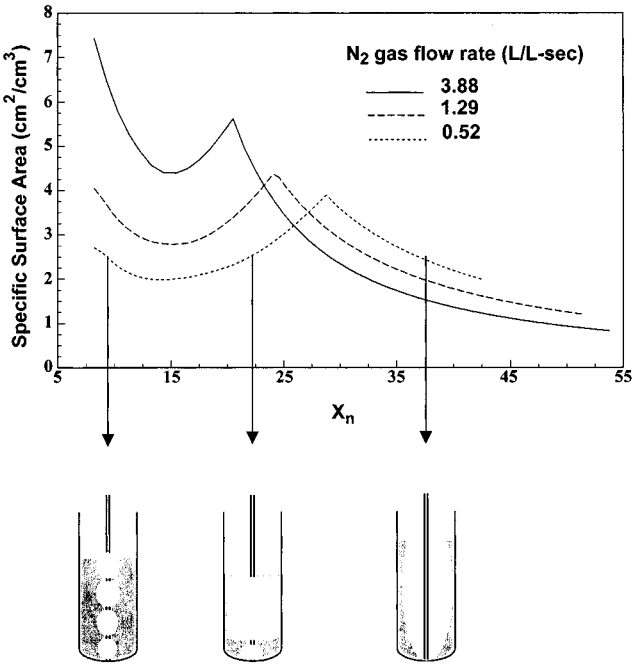

Figure 9. Variation in specific mass-transfer area during polymerization (calculation).

resulting in a decrease in the specific interfacial surface area. There is a period when both large slugs and bubbles coexist and the specific surface area increases. As the reaction progresses further, a large slug rises and bursts, and gas flows through the reactor without forming any bubbles or slugs until the polymer melts flowing down along the reactor tube walls form a pool again. As a result, the specific surface area decreases again. It is interesting to observe in Figure 9 that the

specific surface areas for high gas flow rates are larger than those for low gas flow rates at low conversion. Although the specific surface area is a little larger for low gas flow rates than for high gas flow rates as the polymer molecular weight increases, the overall rate of polymerization or the conversion of functional groups is lower at low gas flow rates. This is because the rate of removal of gas bubbles is also a factor (eq 14).

Concluding Remarks

In this paper, we presented new experimental results on the melt polycondensation of bisphenol A polycarbonate by the forced gas sweeping process. A simple mass-transfer reaction model was also developed. Although our experiments were carried out in a small glass reactor, it has been demonstrated that the polymer molecular weight can be effectively increased in a reasonable reaction time by injecting heated inert gas into a polymer melt. The rate of polymerization seems to be quite comparable to that of a multistage high-vacuum polymerization in a stirred reactor. Both the reaction temperature and the gas flow rate are key process variables for obtaining high polymer molecular weights. The proposed model also provides reasonable predictions of the polymer molecular weight, albeit with several correlations taken from the literature to estimate the effective mass-transfer area. The correlations that we used to calculate the bubble size and bubble rising velocity were developed and tested for much lower viscosity fluids by the original researchers. Therefore, there is a question of whether such correlations would be valid in our polymerization system where the melt viscosity is much higher and possibly beyond the limits of validity of these correlations. Certainly, more studies on the formation of bubbles and their behavior in a polycarbonate melt would be desirable in the future. Although there is an issue of feasibility of the forced gas sweeping process for scale-up, the proposed polymerization process appears to be a potential alternative to conventional high-vacuum melt polycondensation processes.

Acknowledgment

This work was supported by LG Chemical Company in Taejon, Korea. Laboratory assistance by Michael Mitchell (currently at the University of Illinois) is also appreciated.

Nomenclature

a = specific mass-transfer area (cm^2/cm^3)
d_b = bubble diameter (cm)
C_d = drag coefficient
D_p = diffusivity of phenol in polycarbonate (cm^2/s)
D_R = reactor tube diameter (cm)
$[E_A]$ = concentration of terminal hydroxyl group (mol/cm^3)
$[E_B]$ = concentration of terminal phenyl carbonate group (mol/cm^3)
g = acceleration of gravity (cm/s^2)
k_* = reaction rate constant ($cm^3\ mol^{-1}\ s^{-1}$)
k_L = mass-transfer coefficient (cm/s)
K = vapor−liquid equilibrium coefficient
$\bar{M}_n$ = number-average molecular weight (g/mol)
$\bar{M}_w$ = weight-average molecular weight (g/mol)
N_b = number of gas bubbles
N_p = molar transfer rate of phenol ($mol\ cm^{-3}\ s^{-1}$)
$[P]$ = concentration of phenol (mol/cm^3)
Q_G = gas flow rate (cm^3/s)
Re = Reynolds number
r_p = rate of polymerization ($mol\ L^{-1}\ min^{-1}$)
S_G^* = surface area of a gas bubble (cm^2)
S_R = cross-sectional area of reactor tube (cm^2)
T = temperature (K)
u_b = bubble rising velocity (cm/s)
V_G = total volume of gas bubbles (cm^3)
V_G^* = volume of a single gas bubble (cm^3)
V_L = melt phase volume (cm^3)
$\bar{X}_n$ = number-average degree of polymerization
$\bar{X}_w$ = weight-average degree of polymerization

Greek Letters

ϵ_G = fractional gas fraction
μ = melt viscosity (g-cm/s)
θ = bubble-liquid contact time (s)
ρ = melt density (g/cm^3)

Subscripts

b = bubble
G = gas phase
L = liquid phase
m = polymer melt phase

Literature Cited

(1) Carroll, S. *Chem. Mark. Rep.* **1999**, *Nov 15*, 13.
(2) Kim, Y. S.; Choi, K. Y. Multistage Melt Polymerization of Bisphenol A and Diphenol Carbonate to Polycarbonate. *J. Appl. Polym. Sci.* **1993**, *49*, 747.
(3) Bhatia, K. K. Apparatus and Process for a Polycondensation Reaction. U.S. Patent 5,856,423, 1999.
(4) Bhatia, K. K. Polyester Production Process. U.S. Patent 5,849,849, 1998.
(5) Bhatia, K. K. Polyester Production Process. U.S. Patent 5,688,898, 1997.
(6) Woo, B. G.; Choi, K. Y.; Goranov, K. The Forced Gas Sweeping Process for Semibatch Melt Polycondensation of Poly(Ethylene Terephthalate). *J. Appl. Polym. Sci.* **2000**, in press.
(7) Hersh, S. N.; Choi, K. Y. Melt Transesterification of Diphenyl Carbonate with Bisphenol A in a Batch Reactor. *J. Appl. Polym. Sci.* **1990**, *41*, 1033.
(8) Kim, Y. S.; Choi, K. Y.; Chamberlin, T. A. Kinetics of Melt Transesterification of Dephenyl Carbonate and Bisphenol A to Polycarbonate with $LiOH{\cdot}H_2O$ Catalyst. *Ind. Eng. Chem. Res.* **1992**, *31*, 2118.
(9) Song, K. H.; Lee, S. H.; Park K. H. Process and Equipment for Preparing High Polymerized Aromatic Polycarbonate Using Horizontal Tubular Reactor. Korean Patent Application 1999-73161, 1999.
(10) Davidson, J. F.; Schüler, B. O. G. Bubble Formation at an Orifice in a Viscous Liquid. *Trans. Inst. Chem. Eng.* **1960**, *38*, S105.
(11) Schnell, H. *Chemistry and Physics of Polycarbonates*; Interscience: New York, 1964; p 124.
(12) Chhabra, R. P. Rising Velocity of a Swarm of Spherical Bubbles in Power Law Fluids at High Reynolds Numbers. *Can. J. Chem. Eng.* **1998**, *76*, 137.
(13) Snabre, P.; Magnifotcham, F. Formation and Rise of a Bubble Stream in a Viscous Liquid. *Eur. Phys. J.* **1998**, *B4*, 369.
(14) Godbole, S. P.; Honath, M. F.; Shah, Y. T. Holdup Structure in Highly Viscous Newtonian and Non-Newtonian Liquids in Bubble Columns. *Chem. Eng. Commun.* **1982**, *16*, 119.
(15) Pell Jr., T. M.; Davis, T. G. Diffusion and reaction in polyester melts. *J. Polym. Sci.: Polym. Phys.* **1973**, *11*, 1671.

Received for review October 23, 2000
Revised manuscript received January 9, 2001
Accepted January 10, 2001

IE000908Y